Biophysical Chemistry 21 (1985) 127–136
Elsevier

BPC 00900

MECHANISM OF THE BINDING OF 2-(4′-HYDROXYPHENYLAZO)BENZOIC ACID TO BOVINE SERUM ALBUMIN

Kiyofumi MURAKAMI, [a] Takayuki SANO, [b] Shiro TSUCHIE [b] and Tatsuya YASUNAGA [b,*]

[a] *Department of Chemistry, Faculty of Science, Yamagushi University, Yoshida 1677-1, Yamaguchi 753 and* [b] *Department of Chemistry, Faculty of Science, Hiroshima University, Higashisenda-machi, Naka-ku, Hiroshima 730, Japan*

Received 22nd March 1984
Revised manuscript received 24th July 1984
Accepted 11th September 1984

Key words: Bovine serum albumin; Relaxation method; Sequential binding

The mechanism of the binding of 2-(4′-hydroxyphenylazo)benzoic acid (HABA) to bovine serum albumin was studied by relaxation methods as well as the binding isotherm using gel chromatography. A single relaxation was observed over a wide range of HABA concentration except at the extremes of high concentration where another slow process was observed. The concentration dependence of the reciprocal relaxation time of the fast process decreased monotonically with increase in concentration of HABA at constant polymer concentration. The data were analyzed on the basis of Brown's domain structure model and were found to be consistent with a sequential binding mechanism. The azohydrazon tautomerism of HABA was identified with the intramolecular step of the complex. The activation parameters of the step, determined from the temperature dependence of the relaxation time of the fast process, showed that this step is rate limited by an enthalpy barrier in both forward and backward directions. Comparison of the activation parameters with those of other serum albumin-ligand systems suggests that there is an enthalpy-entropy compensation in the activation process of the intramolecular step with the compensation temperature at about 270 K; the enthalpy-entropy compensation is thought to be related to the hydrophobic nature of the ligand.

1. Introduction

Serum albumin reversibly binds many kinds of physiologically and clinically important small organic molecules such as fatty acids, bilirubin, amino acids, drugs and hormones, and acts as a carrier of and a buffer to those molecules in the body, which is important with respect to the determination of the distribution, activity, metabolism and excretion of these molecules [1–3]. For these reasons, the binding of small organic molecules with serum albumin has been extensively studied. The majority of these studies, however, have been concerned only with the determination of the number of binding sites and the binding constants, so that the detailed binding mechanisms have scarcely been established.

However, some developments have recently been made in this area. One of these is the identification of the binding site in the amino acid sequence by the method of combining affinity labeling with amino acid sequence determination through peptic or tryptic digestion or through reduction by cyanogen bromide [4–8]. Another is the clarification of the binding mechanism using kinetic methods such as the stopped-flow [9–15], temperature-jump [16], and pressure-jump methods [17]. Combining these results with Brown's [18] three-dimensional model of domain structure, it has been

* To whom correspondence should be addressed.

Abbreviations: HABA, 2-(4′-hydroxyphenylazo)benzoic acid; BSA, bovine serum albumin; HSA, human serum albumin; D_0/P_0, ratio of initial concentration of dye to that of polymer.

recognized that an organic anion binds to serum albumin generally in a multi-step mechanism: the first step is the bimolecular binding reaction to form a complex in which the ligand is attached probably to the cation-rich surface portion located at the mouth of the hydrophobic hole, and the subsequent steps are the stabilization processes of the complex, i.e., the migration of the ligand into the hydrophobic hole. In spite of these investigations, information is still lacking, especially with regard to the possibility of an interaction between binding sites. In most studies of binding isotherms, independency between binding sites is assumed [19] unless an explicit positive cooperativity is observed. Only kinetic studies over a wide range of ligand concentrations may elucidate the manner of the interaction between primary and secondary binding sites.

HABA, which has frequently been used as a convenient spectrophotometric probe for albumin binding of many kinds of drugs [20–24], binds to serum albumin, exhibiting a metachromasy band at around 480 nm at the expense of the original band at 350 nm [25]. Moriguchi et al. [26] and Terada et al. [27] have ascribed the origin of the metachromasy to the azo-hydrazone tautomerism of HABA induced by the binding to a hydrophobic site. On the other hand, the binding isotherm [25] shows the existence of at least two kinds of binding sites. Assuming that both binding sites are independent of each other, Sakurai et al. [28] have assigned the high- and low-affinity sites to the metachromasy (hydrazone) and the non-metachromasy (azo) sites, respectively. Furthermore, from studies of the effects of drugs on the induced circular dichroism spectra of the HABA-BSA complex, these workers [29,30] have suggested three kinds of bound species (two azo forms and one hydrazone form) under the assumption that the stacking of the bound HABA and the conformational change of BSA with increase in D_0/P_0 are negligible. Considering that the validity of these assumptions has not been established, it is desirable to clarify the detailed binding mechanism from a kinetic point of view. Such a study will provide a basis for the use of HABA as a spectrophotometric probe and for the studies referred to above.

In this report the mechanism of the binding of HABA to BSA, with respect to the relationship between the primary and secondary binding sites, is investigated over a wide range of dye concentration by temperature-jump and pressure-jump methods, as well as by the binding isotherm using gel chromatography. The data are analyzed on the basis of the domain structure model of Brown [18] and are found to be consistent with a sequential binding mechanism. The activation parameters of the conformational change subsequent to the bimolecular binding step are discussed in comparison with those of other serum albumin-ligand systems.

2. Experimental procedure

2.1. Materials

BSA fraction V (lot No. LTH3715) was purchased from Wako Pure Chemical Industries and used without further purification. The dimer content was about 5%, as determined by gel chromatography with Sephadex G-150. The fatty acid content was determined to be 0.33 mol/mol albumin by the method of Dole [31]. The molar concentration was determined from the absorbance at 280 nm ($E^{1\%}_{1\,cm} = 6.6$ [32]), assuming a molecular weight of 67000. HABA (purity not less than 98%) was purchased from Eastman Kodak Co. The degree of the proton dissociation of the hydroxyl group was determined to be 3.7% at pH 7.0 from the pK value (8.43) which was obtained from a combination of a spectrophotometric titration and a nonlinear least-square fit analysis. The concentration dependence of the absorbance was found to obey Beer's law up to 1×10^{-3} M. These facts indicate that HABA exists in the negatively charged monomer form under the present experimental conditions. Other chemicals used were reagent grade. All the sample solutions were prepared in 0.1 M phosphate buffer at pH 7.00 ± 0.02.

2.2. Methods

Absorption spectra were measured with an Union Giken SM401 spectrophotometer. The binding

isotherm was determined by gel chromatography [33] with Sephadex G-25. The data were analyzed by the method of Scatchard [19].

Kinetic studies were performed using the joule heating temperature-jump apparatus and the pressure-jump apparatus, both of which were constructed in our laboratory [34,35]. The light source used was a halogen lamp (250 W) and the path length of the cell was 10 mm. The rise time and the magnitude of the temperature jump were 5 μs and 6°C, respectively. In the case of the pressure jump, a pressure decrease of about 80 atm was obtained within 100 μs by rupture of a brass diaphragm. All measurements were performed at 25 ± 0.2°C with the exception of the study on activation parameters.

3. Results

3.1. Binding isotherm

Fig. 1 illustrates a Scatchard plot of the binding of HABA to BSA at pH 7.0 and 25°C. This binding isotherm reveals the existence of at least two classes of binding sites. On the assumption of independent sites, a least-square fit analysis yields the binding parameters: $n_1 = 2.7$, $K_1 = 1.54 \times 10^4$ M^{-1}, $n_2 = 6.6$, $K_2 = 5.2 \times 10^2$ M^{-1} where n and K are the number of binding sites and the binding constant, and 1 and 2 refer to the primary and the secondary binding sites, respectively. As can be seen in fig. 1, the observed data fall on the theoretical curve calculated using these values. Hence, it can be seen that a total amount of at least nine HABA molecules are able to bind per molecule of BSA.

The binding of HABA to BSA has also been investigated using equilibrium dialysis [25], rotating-disk polarography, ultrafiltration [36], and spectrophotometric titration methods [37]. Although the binding isotherms reported in the former two studies agree well with the present results in their profiles, the binding parameters were not estimated. On the other hand, Terada et al. [37] have reported values of $n = 1.8$ and $K = 2.7 \times 10^4$ M^{-1}. The differences of these values from those of the present study are probably due to the assumption of only one kind of bound species in their study (cf. ref. 28).

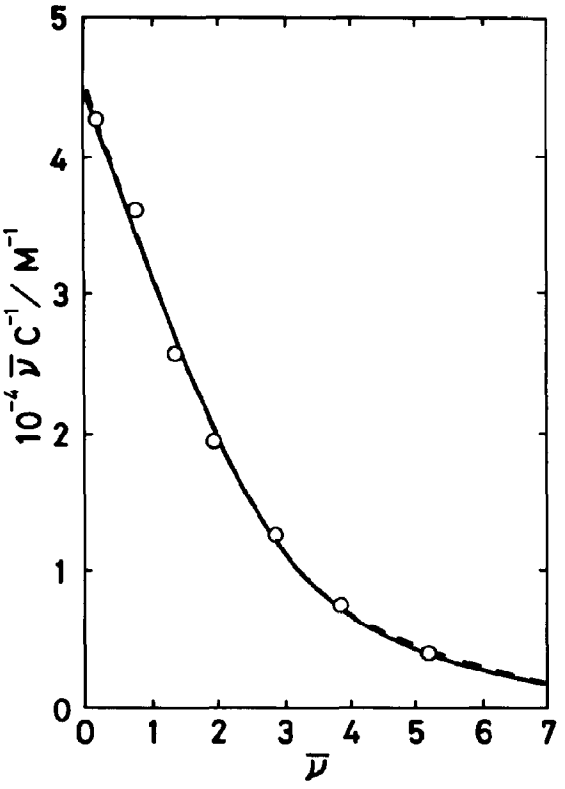

Fig. 1. Scatchard plot of the binding of HABA to BSA at 25°C. (O) Observed data; (— — —) theoretical curve calculated using the values of the binding parameters listed in the text. (———) Reconstructed binding isotherm based on the mechanism of eq. 8 (see text for details).

3.2. Characteristics of the relaxation signal

A single relaxation (time range 20–40 ms) was observed in both pressure-jump and temperature-jump measurements over the entire concentration range except at high HABA concentrations, where a double relaxation including another slow process was observed with the pressure-jump method. The direction of the relaxation signal at 480 nm corresponds to a decrease in the absorbance of the solution. At wavelengths lower than 395 nm, relaxations of opposite direction were observed. This

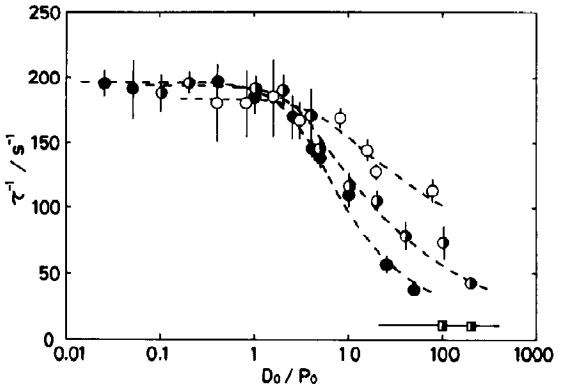

Fig. 2. D_0/P_0 dependence of the reciprocal relaxation times at several BSA concentrations. Fast process: (○) 1.25×10^{-5} M, (○) 5×10^{-5} M, (●) 2×10^{-4} M; slow process: (■) 5×10^{-5} M. The dashed lines are drawn to emphasize the tendency of the fast process. The solid line represents the theoretical one of eq. 10 using the values of parameters cited in the text.

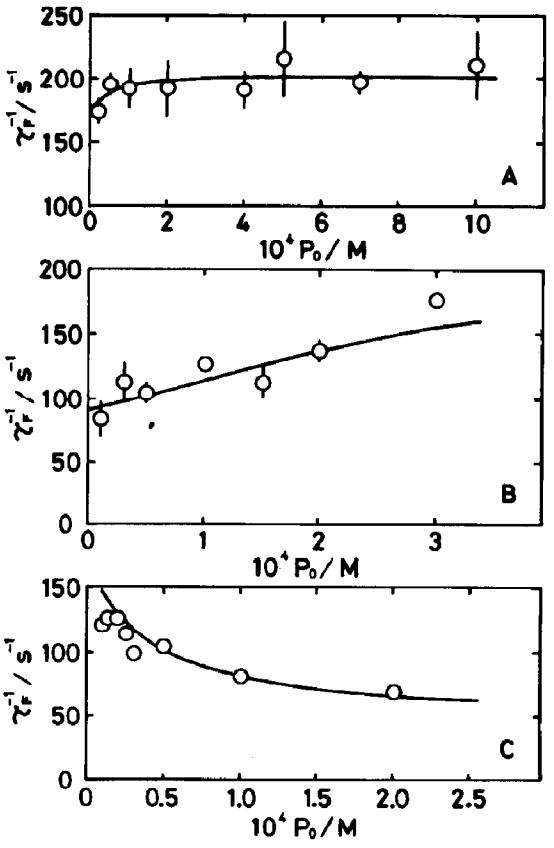

Fig. 3. Concentration dependences of the reciprocal relaxation time of the fast process. (A) BSA concentration dependence in the D_0/P_0 region below unity at $[HABA]=1\times10^{-5}$ M. (B) BSA concentration dependence in the D_0/P_0 region above unity at $[HABA]=1\times10^{-3}$ M. (C) Concentration dependence at $D_0/P_0=20$. (———) Calculated curves based on the mechanism of eq. 8 using the values of the parameters cited in the text.

behavior of the relaxation signal indicates that the equilibrium shifts toward dissociation of the complex with a decrease in pressure. In the case of the temperature-jump, the equilibrium shifts toward dissociation with an increase in temperature. The values of the relaxation times from both measurements agreed well with each other. Fig. 2 shows the D_0/P_0 dependence of the reciprocal relaxation time at several BSA concentrations. As can be observed in this figure, the reciprocal relaxation time of the fast process decreases with increase in D_0/P_0 for all cases. In addition, data for the relaxation time of the fast process, the concentration dependences of the fast relaxation process at D_0/P_0 above and below unity and at constant D_0/P_0, were measured. The results are shown in fig. 3. On the other hand, the reciprocal relaxation time of the slow process does not depend on D_0/P_0, although the observable concentration range is not sufficiently wide.

One additional very rapid change in the absorbance was observed outside the time resolution of the apparatus. From the concentration and wavelength dependences of its amplitude (i.e., the amplitude was proportional to the concentration of free HABA and the wavelength dependence was consistent with the absorbance change of free HABA against pH) the origin of this effect was attributed to the proton dissociation reaction of free HABA. No other effect attributable to the binding between HABA and BSA was observed.

3.3. Examination of the reaction mechanism

Kinetic studies, which have hitherto been performed for the binding of small molecules to serum albumin, have mainly been concerned with the primary binding site. The following types of mech-

anisms have been proposed [10,12–17,38]

$$L + P \rightleftharpoons C \quad (1)$$

$$L + P \rightleftharpoons C_1 \rightleftharpoons C_2 \quad (2)$$

$$L + P \rightleftharpoons C_1 \rightleftharpoons C_2 \rightleftharpoons C_3 \quad (3)$$

$$L + P \rightleftharpoons C_1 \rightleftharpoons C_2 \rightleftharpoons C_3 \rightleftharpoons C_4 \quad (4)$$

$$L + P \rightleftharpoons C_1 \rightleftharpoons C_2 \rightleftharpoons C_3 \rightleftharpoons C_4 \rightleftharpoons C_5 \quad (5)$$

where L, P, and C_i denote free ligand, free primary binding site, and complex, respectively. These models consist of a binding step and subsequent conformational change of the complexes. As is well known [39], the reciprocal relaxation time for any step in these models can be expressed by an increasing function of the sum of concentrations of the free ligand and the free binding site. For the present system, on the basis of the binding parameters described previously, the sum of the concentrations of free ligand and binding site increases with D_0/P_0 at $D_0/P_0 \geqq 4$. If the present relaxation is ascribed to any step in the above mechanisms, the reciprocal relaxation time should increase with D_0/P_0 above 4. The observed results (fig. 2) are not consistent with this expectation; therefore, these types of mechanisms can be excluded from the possible ones. From a similar consideration, the next type of model [40], in which the primary and secondary binding sites compete with each other for the ligand, can also be excluded.

$$\begin{aligned} L + P_1 &\rightleftharpoons C_1 \\ L + P_2 &\rightleftharpoons C_2 \end{aligned} \quad (6)$$

An alternative model is to introduce an interaction between primary and secondary binding sites. According to Brown [18], BSA consists of three domains, each of which is constructed of five or six helix columns forming a cylinder-like structure and its hydrophobic inner side is proposed to form the binding site of organic anions. Assuming that each domain is identical and independent for ligand binding and sequentially binds two ligands through a conformational change of the complex, the next sequential binding mechanism was applied to the present system.

$$\begin{array}{ccccccc} & & K_1 & & K_2 & & K_3 \\ & & D & & k_{2F} & & D \\ P & \longleftarrow & & \longrightarrow C_1 & \longleftrightarrow & C_2 & \longleftarrow \\ & & & & k_{2B} & & \end{array} \quad C_3 \quad (7)$$

very fast fast very fast

where P and D denote free domain and free dye, respectively. Assuming that the binding reactions are rapid relative to the conformational change, this type of mechanism can principally describe the present kinetic behavior of the fast process [41]. Furthermore, taking account of the existence of another slow relaxation at high concentrations of HABA and nine binding sites per protein (three sites per domain), the mechanism denoted by eq. 7 was modified as

$$\begin{array}{ccccccccc} & & K_1 & & K_2 & & K_3 & & K_4 \\ & & D & & k_{2F} & & D & & k_{4F} \\ P & \longleftarrow & & \longrightarrow C_1 & \longleftrightarrow & C_2 & \longleftarrow & \longrightarrow C_3 & \longleftrightarrow \\ & & & & k_{2B} & & & & k_{4B} \end{array} \quad C_4 \quad (8)$$

very fast fast very fast slow

$$D + P' \overset{K_5}{\longleftrightarrow} C_5$$

very fast

where P′ denotes an additional binding site in the domain. The binding of HABA to P′ is independent of the upper line in eq. 8 except for the coupling through free HABA. This is the simplest model which is consistent with the observed kinetic and equilibrium data. Under the assumption of rapid equilibration of the binding reactions, the reciprocal relaxation time of the fast process can be expressed by

$$\tau_F^{-1} = k_{2F}G + k_{2B}H \quad (9)$$

with

$$\begin{aligned} G = \{ & K_1(D+P) + K_1K_3D(D+2P+C_2) \\ & + K_1K_5D(D+P+P') + K_1K_3K_5D^2 \\ & \times (D+2P+P'+C_2)\}/\{1 + K_1(D+P) \\ & + K_3(D+C_2) + K_5(D+P') \\ & + K_1K_3D(D+P+C_2) + K_1K_5D(D+P+P') \\ & + K_3K_5D(D+P'+C_2) \\ & + K_1K_3K_5D^2(D+P+P'+C_2)\} \end{aligned}$$

$$H = \{1 + K_1(D+P) + 2K_3C_2 + K_5(D+P') + K_1K_3DC_2 + K_1K_5D(D+P+P') + 2K_3K_5DC_2 + K_1K_3K_5D^2C_2\}/\{1 + K_1(D+P) + K_3(D+C_2) + K_5(D+P') + K_1K_3D(D+P+C_2) + K_1K_5D(D+P+P') + K_3K_5D(D+P'+C_2) + K_1K_3K_5D^2(D+P+P'+C_2)\}$$

and that of the slow process becomes

$$\tau_S^{-1} = k_{4F}I + k_{4B} \qquad (10)$$

where

$$I = [K_1K_2K_3D^2\{1 + K_5(D+P')\} + 4(1 + K_5D) \times K_3C_2 + K_1(1+K_2)(1+K_5D)C_3]/[\{1 + K_1(1+K_2)D + K_1K_2K_3D^2\} \times \{1 + K_5(D+P')\} + 4 + (1+K_5D)K_3C_2 + K_1(1+K_2)(1+K_5D)(P+C_3)]$$

The observed data were fitted to eqs. 9 and 10. By calculating the equilibrium concentrations of each species for a set of assumed values of the parameters, the concentration dependences of τ_F^{-1} and τ_S^{-1} can be estimated. The binding isotherm can also be constructed from the equations $\bar{\nu} = (C_1 + C_2 + 2C_3 + 2C_4 + C_5)/3P_0$ and $\bar{\nu}C^{-1} = \bar{\nu}/D$. Among many sets of assumed values of the parameters, the best fit one was chosen so as to minimize the deviations of the theoretically calculated D_0/P_0 dependences of reciprocal relaxation times τ_F^{-1} and τ_S^{-1}, and reconstructed binding isotherm from those observed, at the same time. The best fit

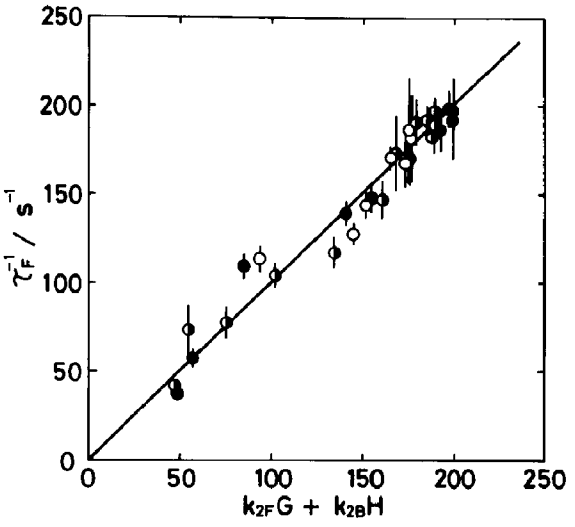

Fig. 4. Plot of the observed reciprocal relaxation time of the fast process vs. $k_{2F}G + k_{2B}H$ calculated using the values of parameters cited in the text. The solid line is that which has a slope equal to unity and passes through the origin. If the mechanism and the values of the parameters are correct, the observed data must fall on this line.

curves are shown as the unbroken lines in fig. 4 (τ_F^{-1}), fig. 2 (τ_S^{-1}) and fig. 1 (binding isotherm), which were calculated using the values: $K_1 = 1.16 \times 10^4$ M^{-1}, $K_2 = 0.24$ ($k_{2F} = 40$ s^{-1}, $k_{2B} = 165$ s^{-1}), $K_3 = 2.0 \times 10^3$ M^{-1}, $K_4 = 0.1$ ($k_{4F} = 1.0$ s^{-1}, $k_{4B} = 11$ s^{-1}), $K_5 = 500$ M^{-1}; all the curves are in good agreement with the experimental data. To add confidence to these values, other kinds of concentration dependences of the reciprocal relaxation time of the fast process were calculated using these values, and were compared with the

Table 1

Kinetic and thermodynamic parameters for the sequential binding mechanism (eq. 8)

Step	K_i	k_{iF} (s^{-1})	k_{iB} (s^{-1})	$\Delta H_{iF}^{\ddagger}$ (kJ mol^{-1})	$\Delta S_{iF}^{\ddagger}$ (J K^{-1} mol^{-1})	$\Delta H_{iB}^{\ddagger}$ (J mol^{-1})	$\Delta S_{iB}^{\ddagger}$ (J K^{-1} mol^{-1})
1	11600 ± 500 M^{-1}						
2	0.24 ± 0.04	40 ± 5	165 ± 5	48.5 ± 5.1	−48.1 ± 17.4	58.0 ± 4.1	−9.9 ± 13.9
3	2000 ± 400 M^{-1}						
4	≦ 0.4	≦ 3	8–12				
5	450 ± 50 M^{-1}						

observed data in fig. 3 (unbroken lines); the calculated constants also reproduced well these concentration dependences of the fast process. The values of the parameters are listed in table 1.

3.4. Thermodynamic parameters

The activation parameters of the fast conformational change were determined from the temperature dependence of the relaxation time of the fast process. The measurements were performed for the following two conditions: (A) [BSA] = 7×10^{-4} M, [HABA] = 1×10^{-5} M, and (B) [BSA] = 5×10^{-5} M, [HABA] = 5×10^{-3} M.

Substituting the values of the equilibrium constants obtained in the previous section in eq. 9, the reciprocal relaxation time can be rewritten as $\tau_F^{-1} = 0.982k_{2F} + 0.099k_{2B}$ for sample B. By further substitution of the values of the rate constants, it can be seen that the first term is predominant. Hence, we can regard the temperature dependence of the reciprocal relaxation time of sample B as that of k_{2F} to a first approximation. Subtracting the second term from τ_F^{-1} and dividing by the coefficient of k_{2F}, we obtain the Eyring plot of k_{2F} from which the activation enthalpy and entropy can be calculated. Applying the same procedure to eq. 9 for the reciprocal relaxation time of sample A, $\tau_F^{-1} = 0.923k_{2F} + 1.000k_{2B}$, and further substitution shows the second term to be predominant. In this case the temperature dependence of k_{2B} can be obtained by subtracting the first term, the temperature dependence of which has already been estimated in the previous step, from τ_F^{-1} for each temperature and dividing by the coefficient of k_{2B}. Thus calculated, the temperature dependence of k_{2B} was used in the recalculation of that of k_{2F} for sample B. This procedure was repeated until the activation parameters converged. The resultant Eyring plots of the rate constants are shown in fig. 5; the solid lines represent the least-square fits to the data. From the slope and intercept, the activation enthalpy and entropy of the forward and backward reactions were determined, respectively. These results are also summarized in table 1.

From the activation parameters, the standard free energy change of the fast conformational

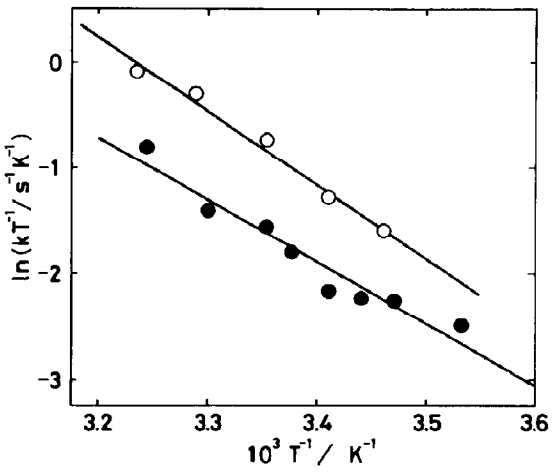

Fig. 5. Eyring plot of the forward (●) and backward (○) rate constants of the second step in eq. 8. See text for details.

change ΔG_2 could be determined to be 1.96 kJ mol^{-1} using the equation

$$\Delta G_2 = \Delta G_{2F}^{\neq} - \Delta G_{2B}^{\neq} = (\Delta H_{2F}^{\neq} - T\Delta S_{2F}^{\neq}) - (\Delta H_{2B}^{\neq} - T\Delta S_{2B}^{\neq}) \quad (11)$$

where $\Delta G_{2F}^{\neq}$ and $\Delta G_{2B}^{\neq}$ represent activation free energies. The equilibrium constant of this step can also be evaluated as $K_2 = \exp(-\Delta G_2/RT) = 0.45$; this is in good agreement with that obtained by the analyses of the relaxation times and the binding isotherm. This agreement shows self-consistency of the present analyses and confirms the validity of the proposed mechanism.

4. Discussion

Both the static and kinetic data support well the sequential binding mechanism of eq. 8 based on the three-dimensional domain structure model of albumin proposed by Brown [18] in which an organic anion binds to the cylindrical hydrophobic hole formed by a pair of face-to-face triple helical troughs (subdomain) forming an electrostatic bond with the cationic groups located at the mouth of the hydrophobic hole. The present assignment of the binding site of HABA to the hydrophobic hole

is consistent with the results of Moriguchi et al. [26] and Terada et al. [27]. The most important feature of eq. 8 is that a secondary binding site is produced by the conformational change of the complex which occurs as a result of the binding of HABA at the hydrophobic hole. This secondary site may be thought of as: either (1) a new site at a different location from that of the first one, for instance, created by exposing a hydrophobic area of the protein; or (2) a result of the migration of the first dye into the hydrophobic hole, leaving a site for the next dye at the original position of the first dye. In the latter case the first dye may form a part of the secondary site. The small entropy change obtained for this process seems to suggest that the latter case is preferable, since a large entropy change would be expected in exposing a hydrophobic area of a protein.

The combination of the mechanism determined in this study and Brown's domain model allows us to visualize the detailed processes of the tautomerism of HABA from the azo to hydrazone form in the following way: At first, HABA binds to albumin at a very rapid rate to form complex C_1 in eq. 8. Considering that no relaxation effect attributable to the bimolecular binding process was observed and that the extinction coefficient of HABA in C_1 is equal or almost equal to that of the free state, then HABA in C_1 can be considered to be in the azo form. This is reasonable, assuming that HABA is attached to the cationic groups on the surface of the protein, i.e., HABA is expected to be in the azo form in a polar environment. Subsequently, complex C_1 relaxes into C_2. The spectral change accompanying this process shows that HABA is in the hydrazone form in C_2. Accounting for the relationship between the tautomerism of HABA and the polarity of its environment, i.e., the hydrazone form prefers a nonpolar environment [26], it can be concluded that the second step is the migration of HABA from the mouth to the interior of the hydrophobic hole. The secondary bound HABA in complex C_3 must take the azo form for the same reason as that of the first dye in C_1. Finally, complex C_3 relaxes into C_4. In this step, the secondary bound dye probably migrates into the hydrophobic region to some extent and, hence, may take the hydrazone form. The number of bound species proposed in the present study is consistent with the results of Sakurai et al. [29,30], i.e., the presence of at least two kinds of azo forms and one hydrazone form. However, on the basis of the results and analysis in the present study, it may be concluded that the assumptions made by Sakurai et al. [28–30], i.e., (1) independence between binding sites and (2) the possibility of stacking bound dyes and conformational change of BSA with D_0/P_0 being negligible, are not necessarily appropriate.

Comparing the values of the activation enthalpies of the second step ($\Delta H^{\neq}_{2F} = 48.5$ kJ mol^{-1}, $\Delta H^{\neq}_{2B} = 58.0$ kJ mol^{-1}) with those of the activation entropies expressed in terms of energy ($-T\Delta S^{\neq}_{2F} = 14.3$ kJ mol^{-1}, $-T\Delta S^{\neq}_{2B} = 3.0$ kJ mol^{-1}), it can be seen that the conformational change of the present system is rate limited by an enthalpy barrier in both forward and backward directions, i.e., several bonds are broken in the activation process without major rearrangement of the configuration of the complex and/or its solvent environment. The activation parameters in the HSA-warfarin system [14] take similar values ($\Delta H^{\neq}_{2F} = 54.8$ kJ mol^{-1}, $-T\Delta S^{\neq}_{2F} = 8.0$ kJ mol^{-1}: these are recalculated values from the original literature) and suggest a similar mechanism. In contrast to these systems, the conformational changes in the systems of HSA-oleate [13] and HSA-hemin [15] are rate limited by entropy barriers ($\Delta H^{\neq}_{2F} = 0$ kJ mol^{-1}, $-T\Delta S^{\neq}_{2F} = 66.8$ kJ mol^{-1} in HSA-oleate and $\Delta H^{\neq}_{2F} = 21.9$ kJ mol^{-1}, $-T\Delta S^{\neq}_{2F} = 48.9$ kJ mol^{-1} in HSA-hemin). The large negative entropies of activation in these systems imply highly ordered activated structures, and have been interpreted as a particularly improbable configuration of the protein [13] or a conformational folding [14], or by an ordering of solvent water exposed to a temporarily accessible additional hydrophobic interface [13]. However, such ordering effects are minimal in the present and HSA-warfarin systems compared to the activation entropies as mentioned above. It is further noticeable that in spite of these differences in activation enthalpy and activation entropy between ligands, the activation free energy is almost constant from ligand to ligand ($\Delta G^{\neq}_{2F} = 63$–$71$ kJ mol^{-1}). This fact seems to suggest an enthalpy-

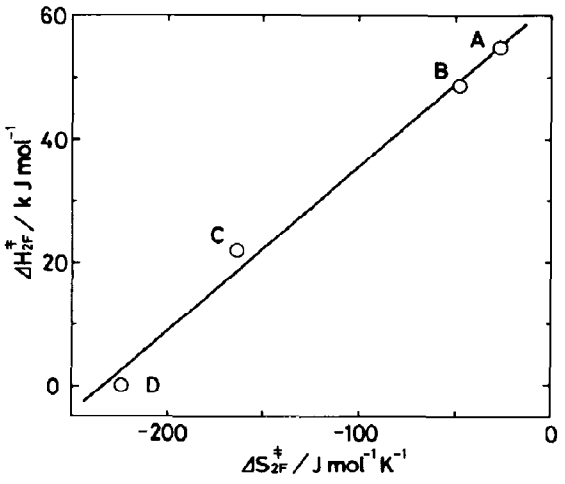

Fig. 6. Enthalpy-entropy compensation pattern in the activation process of the forward reaction of the second step observed for various serum albumin-ligand systems. (A) HSA-warfarin, (B) BSA-HABA, (C) HSA-haemin, (D) HSA-oleate. The solid line represents the least-square fit to the data, the slope of which gives the compensation temperature, 267.3 K.

entropy compensation in the activation process of the second step. Fig. 6 shows the compensation pattern which gives compensation temperature of 267 K. Considering the hydrophobicities of these ligands, this compensation behavior (the distribution of the activation free energy between enthalpy and entropy terms) seems to be closely related to the hydrophobic nature of ligand. That is, the larger the hydrophobicity, the larger the negative activation entropy becomes and the smaller the activation enthalpy. In this connection, Lumry and Rajender [42] have suggested that the hydration properties of solutes play a central role in enthalpy-entropy compensation phenomena. If our suggestion as to the relation between the order on the compensation line in fig. 6 and the hydrophobicity of a ligand is correct, the reverse order between BSA-HABA and HSA-warfarin systems of that expected by a consideration of the hydrophobicities of these ligands may be attributed to a difference in hydration state between BSA and HSA. Concerning the role of the ligand in the activated configuration, we may conclude that the distribution of the activation free energy between enthalpy and entropy terms as well as the activated configuration is closely dependent on the hydrophobicity of ligand, but the magnitude of the activation free energy itself is determined by an inherent property of the serum albumin molecule in water.

References

1 M.C. Meyer and D.E. Guttman, J. Pharm. Sci. 57 (1968) 895.
2 E.M. Sellers and J. Koch-Weser, in: Albumin structure function and uses, eds. V.M. Rosenoer, M. Oratz and M.A. Rothschild (Pergamon Press, New York, 1977) p. 159.
3 P.G. Dayton, Z.H. Israili and J.M. Perel, Ann. N.Y. Acad. Sci. 226 (1973) 172.
4 L.-O. Anderson, A. Rehnström and D.R. Eaker, Eur. J. Biochem. 20 (1971) 371.
5 T.P. King, Ann. N.Y. Acad. Sci. 226 (1973) 94.
6 R.G. Reed, R.R.C. Feldhoff, O.L. Clute and T. Peters, Jr, Biochemistry 14 (1975) 4578.
7 K.K. Gambhir, R.H. McMenamy and F. Watson, J. Biol. Chem. 250 (1975) 6711.
8 W.H. Pearlman and I.F.F. Fong, J. Biol. Chem. 247 (1972) 8078.
9 R.F. Chen, Arch. Biochem. Biophys. 160 (1974) 106.
10 T. Faerch and J. Jacobsen, Arch. Biochem. Biophys. 184 (1977) 282.
11 R.G. Reed, J. Biol. Chem. 252 (1977) 7483.
12 R.D. Gray and S.D. Stroupe, J. Biol. Chem. 253 (1978) 4370.
13 W. Sheider, Proc. Natl. Acad. Sci. USA 76 (1979) 2283.
14 N. Rietbrock and A. Laßmann, Naunyn-Schmiedeberg's Arch. Pharmacol. 313 (1980) 269.
15 P.A. Adams and M.C. Berman, Biochem. J. 191 (1980) 95.
16 A. Froese, A.H. Sehon and M. Eigen, Can. J. Chem. 40 (1962) 1786.
17 K. Murakami, T. Sano and T. Yasunaga, Bull. Chem. Soc. Jap. 54 (1981) 862.
18 J.R. Brown, in: Albumin structure function and uses, eds. V.M. Rosenoer, M. Oratz and M.A. Rothschild (Pergamon Press, New York, 1977) p. 27.
19 G. Scatchard, Ann. N.Y. Acad. Sci. 51 (1949) 660.
20 I. Moriguchi, Chem. Pharm. Bull. 16 (1968) 597.
21 I. Moriguchi, S. Wada and T. Nishizawa, Chem. Pharm. Bull. 16 (1968) 601.
22 R.I. Nazareth, T.D. Sokoloski, D.T. Witiak and A.T. Hopper, J. Pharm. Sci. 63 (1974) 199.
23 R..I. Nazareth, T.D. Sokoloski, D.T. Witiak and A.T. Hopper, J. Pharm. Sci. 63 (1974) 203.
24 H. Zia and J.C. Price, J. Pharm. Sci. 64 (1975) 1177.
25 J.H. Baxter, Arch. Biochem. Biophys. 108 (1964) 375.
26 I. Moriguchi, S. Fushimi, C. Ohshima and N. Kaneniwa, Chem. Pharm. Bull. 18 (1970) 2447.

27 H. Terada, B.-K. Kim, Y. Saito and K. Machida, Spectrochim. Acta A 31 (1975) 945.
28 T. Sakurai, S. Tsuchiya and H. Matsumaru, J. Pharm. Dyn. 4 (1981) 65.
29 T. Sakurai, S. Tsuchiya and H. Matsumaru, J. Pharm. Dyn. 4 (1981) 345.
30 T. Sakurai, S. Tsuchiya and H. Matsumaru, J. Pharm. Dyn. 4 (1981) 451.
31 V.P. Dole, J. Clin. Invest. 35 (1956) 150.
32 E.J. Cohn, W.L. Huges, Jr and J.H. Weare, J. Am. Chem. Soc. 69 (1947) 1753.
33 G.F. Fairclough, Jr and J.S. Fruton, Biochemistry 5 (1966) 673.
34 S. Inoue, J. Sci. Hiroshima Univ. Ser. A 45 (1981) 295.
35 K. Hachiya, M. Ashida, M. Sasaki, H. Kan, T. Inoue and T. Yasunaga, J. Phys. Chem. 83 (1979) 1866.
36 Y.W. Chien, T.D. Sokoloski, C.L. Olson, D.T. Witiak and R. Nazareth, J. Pharm. Sci. 62 (1973) 440.
37 H. Terada, K. Aoki and M. Kamada, Biochim. Biophys. Acta 342 (1974) 41.
38 F.B. Freedman and J.A. Johnson, Am. J. Physiol. 216 (1969) 675.
39 C.F. Bernasconi, Relaxation kinetics (Academic Press, New York, 1976).
40 J.A. Jansen, Acta Pharmacol. Toxicol. 41 (1977) 401.
41 G.M. Loudon and D.E. Koshland, Jr, Biochemistry 11 (1972) 229.
42 R. Lumry and S. Rajender, Biopolymers 9 (1970) 1125.